Inorg. Chem. **2004**, *43*, 1649–1658

Nickel Complexes with New Bidentate P,N Phosphinitooxazoline and -Pyridine Ligands: Application for the Catalytic Oligomerization of Ethylene†

Fredy Speiser,‡ Pierre Braunstein,*,‡ Lucien Saussine,§ and Richard Welter||

Laboratoire de Chimie de Coordination (UMR 7513 CNRS), Université Louis Pasteur, 4 rue Blaise Pascal, F-67070 Strasbourg Cédex, France, Institut Français du Pétrole, Direction Catalyse et Séparation, CEDI René Navarre, BP 3, F-69390 Vernaison, France, and Laboratoire DECMET (UMR 7513 CNRS), Université Louis Pasteur, 4 rue Blaise Pascal, F-67070 Strasbourg Cedex, France

Received September 30, 2003

The phosphinitooxazoline 4,4-dimethyl-2-[1-oxy(diphenylphosphine)-1-methylethyl]-4,5-dihydrooxazole (**9**), the corresponding phosphinitopyridine ligands 2-ethyl-[1′-methyl-1′-oxy(diphenylphosphino)]pyridine (**11**) and 2-ethyl-6-methyl-[1′-methyl-1′-oxy(diphenylphosphino)]pyridine (**12**), which have a one-carbon spacer between the phosphinite oxygen and the heterocycle, and the homologous ligand 2-propyl-[2′-methyl-2′-oxy(diphenylphosphino)]pyridine (**13**), with a two-carbon spacer, were prepared in good yields. The corresponding mononuclear $[NiCl_2(P,N)]$ complexes **14** (P,N = **9**), **15** (P,N = **11**), and **16** (P,N = **12**) and the dinuclear $[NiCl(\mu\text{-}Cl)(P,N)]_2$ **17** (P,N = **13**) Ni(II) complex were evaluated in the catalytic oligomerization of ethylene. These four complexes were characterized by single-crystal X-ray diffraction in the solid state and in solution with the help of the Evans method, which indicated differences between the coordination spheres in the solution and the solid state. In the presence of methylalumoxane (MAO) or $AlEt_3$, only the decomposition of the Ni complexes was observed. However, complexes **14**–**17** provided activities up to 50 000 mol C_2H_4/(mol Ni)·h (**16** and **17**) in the presence of only 6 equiv of $AlEtCl_2$. The observed selectivities for ethylene dimers were higher than 91% (for **14** or **15** in the presence of only 1.3 equiv of $AlEtCl_2$). The activities for **14**–**17** were superior to that of $[NiCl_2(PCy_3)_2]$, a typical dimerization catalyst taken as a reference. The selectivities of the complexes **14**–**17** for ethylene dimers and α-olefins were the same order of magnitude. From the study of the phosphinite **9**/$AlEtCl_2$ system, we concluded that in our case ligand transfer from the nickel atom to the aluminum cocatalyst is unlikely to represent an activation mechanism.

Introduction

Phosphinite ligands find widespread application in homogeneous catalysis,[1,2] notably in asymmetric catalysis owing to the availability of numerous chiral alcohols, which upon reaction with a chlorophosphine in the presence of a base afford phosphinites in good yields.[3−6] Among the best-known examples are the TADDOP-type bisphosphonites **1** developed by Seebach and co-workers[7] and the phosphinitooxazolines **2** recently reported by the groups of Pfaltz[8] and Richards.[9] The TADDOP ligands **1** are used, e.g., in Pd-catalyzed allylic substitutions,[7] whereas the monophosphinite systems **2** lead with great success to the Ir-catalyzed

† Dedicated to Professor E. Dinjus, on the occasion of his 60th birthday, with our warmest congratulations.

* Author to whom correspondence should be addressed. E-mail: braunst@chimie.u-strasbg.fr. Fax: +33 390 241 322.

‡ Laboratoire de Chimie de Coordination (UMR 7513 CNRS), Université Louis Pasteur.

§ Institut Français du Pétrole, Direction Catalyse et Séparation.

|| Laboratoire DECMET (UMR 7513 CNRS), Université Louis Pasteur.

(1) Agbossou, F.; Carpentier, J.-F.; Hapiot, F.; Suisse, I.; Mortreux, A. *Coord. Chem. Rev.* **1998**, *178*−*180*, 1615−1645.
(2) Denis, P.; Croizy, J. F.; Mortreux, A.; Petit, F. *J. Mol. Catal.* **1991**, *68*, 159−175.
(3) Ojima, I.; Clos, N.; Bastos, C. *Tetrahedron* **1989**, *45*, 6901.
(4) Brown, J. M.; Davies, S. G. *Nature* **1989**, *342*, 631−636.
(5) Blaser, H. U. *Chem. Rev.* **1992**, *92*, 935−952.
(6) Ohff, M.; Holz, J.; Quirmbach, M.; Börner, A. *Synthesis* **1998**, 1391−1417.
(7) Seebach, D.; Devaquet, E.; Ernst, A.; Hayakawa, M.; Kühnle, F. N. M.; Schweitzer, W. B.; Weber, B. *Helv. Chim. Acta* **1995**, *78*, 1636.
(8) Blankenstein, J.; Pfaltz, A. *Angew. Chem., Int. Ed.* **2001**, *40*, 4445−4447.

10.1021/ic035132i CCC: $27.50
Published on Web 02/04/2004

enantioselective hydrogenation of terminal olefins[8,9] and to Pd-catalyzed asymmetric alkylations.[9]

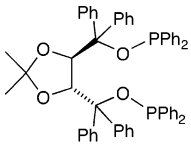

1

TADDOP

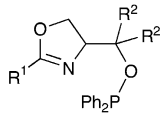

2

R^1 = ferrocenyl, 3,5-*t*-BuC_6H_3, naphthyl
R^2 = *i*-Pr, Bn, *i*-Bu

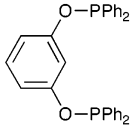

3

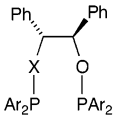

4a X = NCH_3, Ar = Ph
4b X = O, Ar = C_6F_5

The bisphosphinite **3** was recently used with success by Bedford and Welch in the Suzuki coupling reaction of sterically hindered aryls.[10] The bidentate aminophosphine phosphinite ligand **4a** was applied in Pd-catalyzed allylic substitutions,[11] and the bisphosphinite **4b**, in asymmetric Diels−Alder reactions.[12] Notwithstanding these successes,[8,10−12] only a few examples of the applications of phosphinites in oligomerization, polymerization, copolymerization,[13] or hydroformylation reactions have been reported.[14] Thus, for example, Keim and co-workers have used aryl bisphosphinites **5** and **6** in ethylene/CO copolymerization and noted that these ligands show increased stability in comparison to alkyl phosphinites.[13] Phosphinites **7**[15] and **8**[16] have been used in hydroformylation reactions.

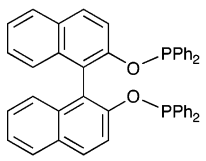

5

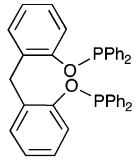

6

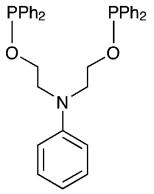

7

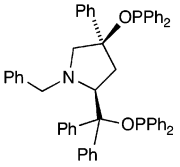

8

To investigate the potential of P,N-type phosphinite ligands in the catalytic oligomerization of ethylene and compare them with phosphinooxazolines and phosphinopyridines that we have recently investigated,[17] we have prepared the new phosphinites **9**−**13** and their respective Ni complexes **14**−**17**, which were used as (pre)catalysts.

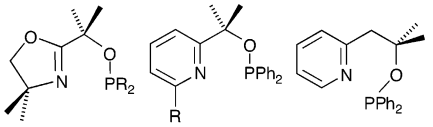

9 R = Ph
10 R = *i*-Pr

11 R = H
12 R = CH_3

13

The basicity of the nitrogen donor will be increased by replacing the oxazoline heterocycle in **9** with a pyridine in **11**−**13**, and we will examine the influence of the ring size of the metal chelate, which increases from six in **15** to seven in **17**, on the nature of the metal coordination sphere and on the catalytic performances.

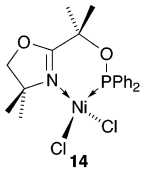

14

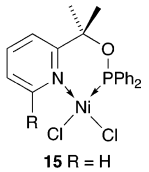

15 R = H
16 R = CH_3

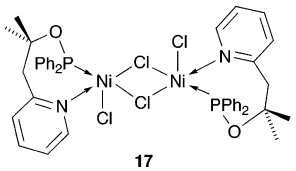

17

Results and Discussion

Synthesis of the Ligands. Phosphinites **9** and **10** were prepared from 2-(4,4-dimethyl-4,5-dihydrooxazol-2-yl)propan-2-ol (**18**), which was readily synthesized by heating 2-hydroxy-2-methylpropionic acid with 2-amino-2-methylpropan-1-ol at 160 °C in xylene.[18] The reaction was completed when no further formation of water was observed in a Dean−Stark trap (eq 1).

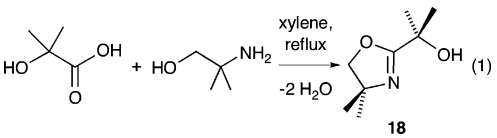

18

The phosphorus group was introduced by lithiation of **18** with 1 equiv of *n*-BuLi to give **19** and subsequent reaction with either PPh_2Cl or borane-protected $P(i\text{-}Pr)_2Cl$. The phosphinitooxazoline **9** was isolated in 76% yield (eq 2). The borane-protected phosphinitooxazoline **20** (eq 3) decomposed during deprotection, which may be due to the strength of the base used ($NHEt_2$) or the possible formation of a stable carbocation upon breaking of the C−O bond.[7]

(9) Jones, G.; Richards, C. J. *Tetrahedron Lett.* **2001**, *42*, 5553−5555.
(10) Bedford, R. B.; Welch, S. L. *Chem. Commun.* **2001**, 129−130.
(11) Gong, L.; Chen, G.; Mi, A.; Jiang, Y.; Fu, F.; Cui, X.; Chan, A. S. C. *Tetrahedron: Asymmetry* **2000**, *11*, 4297−4302.
(12) (a) Bruin, M. E.; Kündig, E. P. *Chem. Commun.* **1998**, 2635−2636. (b) Kündig, E. P.; Saudan, C. M.; Bernardinelli, G. *Angew. Chem., Int. Ed.* **1999**, *38*, 1219−1223.
(13) Keim, W.; Maas, H. *J. Organomet. Chem.* **1996**, *514*, 271−276.
(14) Ungváry, F. *Coord. Chem. Rev.* **1999**, *188*, 263−296.
(15) Kostas, I. D. *J. Organomet. Chem.* **2001**, *626*, 221−226.
(16) Fuerte, A.; Iglesias, M.; Sánchez, F. *J. Organomet. Chem.* **1999**, *588*, 186−194.
(17) (a) Speiser, F. Ph.D. Thesis, Université Louis Pasteur, Strasbourg, France, 2002. (b) Speiser, F.; Braunstein, P.; Saussine, L.; Welter, R. *Organometallics* **2004**, in press. (c) Speiser, F.; Braunstein, P.; Saussine, L. *Organometallics* **2004**, in press.
(18) Pridgen, L. N.; Miller, G. M. *J. Heterocycl. Chem.* **1983**, *20*, 1223−1230.

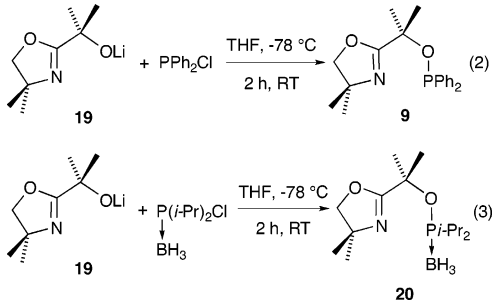

However, **20** can be stored under an inert atmosphere without decomposition.

The synthesis of the phosphinitopyridines **11**−**13** required, first, the metalation of either 2-bromopyridine, 2-bromo-6-methylpyridine,[19] or α-picoline with 1 equiv of *n*-BuLi, followed by the addition of an excess of acetone to give 2-pyridin-2-ylpropan-2-ol (**21**),[20−22] 2-(6-methylpyridin-2-yl)-propan-2-ol (**22**),[20−22] or 2-methyl-1-pyridin-2-ylpropan-2-ol (**23**) in yields of 60, 70, and 71%, respectively, after vacuum distillation (eqs 4 and 5).

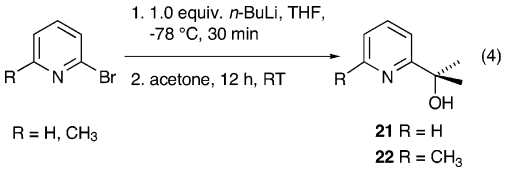

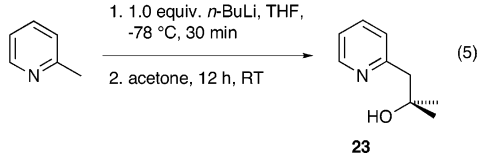

The phosphorus moiety was then introduced by lithiation at −78 °C and subsequent reaction with 1 equiv of PPh_2Cl. After workup, the pyridinyl phosphinites **11**−**13** were isolated in 80, 91, and 85% yields, respectively, as transparent yellow oils, which solidified upon standing for a longer period of time.

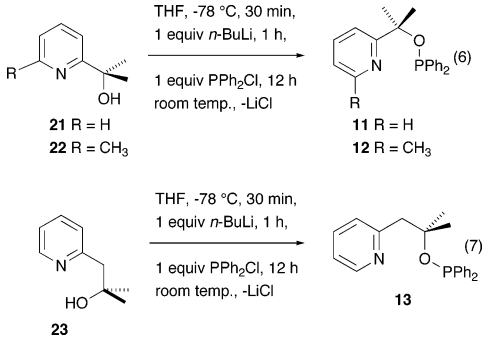

Synthesis of the Nickel Complexes. The nickel(II) phosphinitopyridine complexes **14**−**17** were prepared by the reaction of equimolar amounts of [$NiCl_2$(DME)] with the corresponding ligand for 12 h in CH_2Cl_2 at 25 °C. After workup, the Ni complexes were isolated in 64−79% yields (eqs 8−10). All of the complexes were paramagnetic and were therefore best characterized by X-ray diffraction (Figures 1−4). These structure determinations allowed one to appreciate the differences resulting from changes in the ring size and substituents brought about by the various ligands. The coordination of ligand **9** in **14** was indicated in

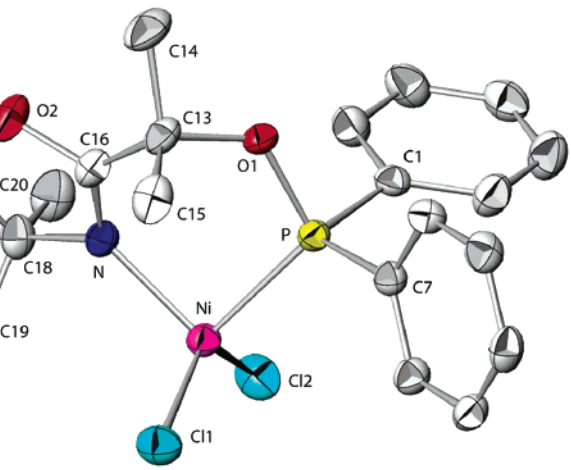

Figure 1. View of the molecular structure of **14** with thermal ellipsoids drawn at the 50% probability level.

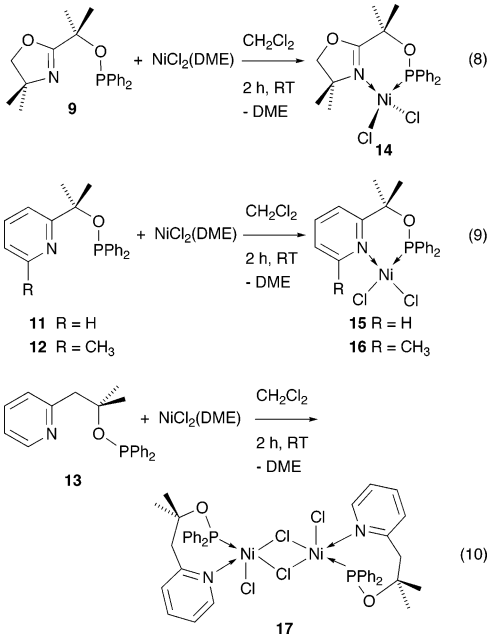

infrared spectroscopy by the shift of the ν_{CN} absorption from 1661 cm^{-1} (free ligand) to 1630 cm^{-1} (coordinated ligand). Similarly, a comparison of the IR data obtained between ligands **11**−**13** and the corresponding complexes **15**−**17** shows that the heterocyclic nitrogen is always coordinated to the metal center (Table 1).[23] The X-ray structure of **14** (Figure 1) shows a distorted, tetrahedral-coordination ge-

(19) Wang, Z.; Reibenspies, J.; Motekaitis, R. J.; Martell, A. E. *J. Chem. Soc., Dalton Trans.* **1995**, 1511−1518.
(20) Tsukahara, T.; Swenson, D. C.; Jordan, R. F. *Organometallics* **1997**, *16*, 3303−3313.
(21) Pasquinet, E.; Rocca, P.; Marsais, F.; Godard, A.; Quéguiner, G. *Tetrahedron* **1998**, *54*, 8771−8782.
(22) Trécourt, F.; Breton, G.; Bonnet, V.; Mongin, F.; Marsais, F.; Quéguiner, G. *Tetrahedron* **2000**, *56*, 1349−1360.

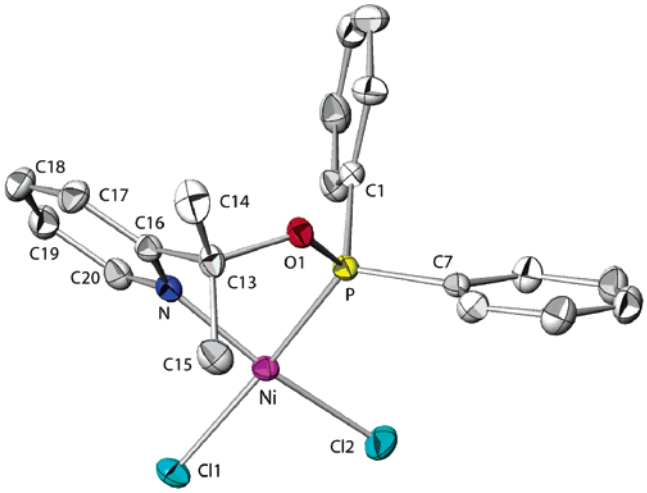

Figure 2. View of the molecular structure of **15** with thermal ellipsoids drawn at the 50% probability level.

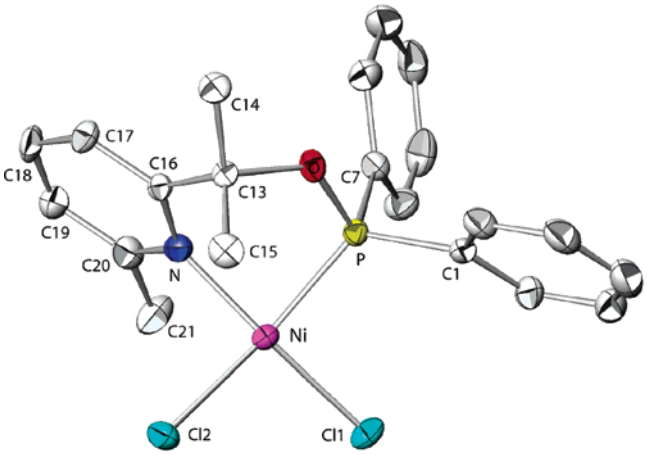

Figure 3. View of the molecular structure of **16** with thermal ellipsoids drawn at the 50% probability level.

ometry for the metal center, and selected bond distances and angles are given in Table 2. The six-membered chelate ring shows a distorted boatlike conformation with the Ni atom and Cl1 out of the P−O−C13−N plane. The opening of the Cl1−Ni−Cl2 angle [125.71(3)°] compared to that in a regular tetrahedron is accompanied by a closing of the N−Ni−P angle.

In contrast to the situation in **14**, the X-ray structure of **15** shows a slightly distorted square-planar-coordination geometry for the Ni atom (Figure 2 and Table 3). The Ni atom is in the mean plane passing through Cl1, Cl2, N, and P [distance 0.0(3) Å]. The sum of the bond angles around Ni is 360.69°. However, a magnetic moment of 2.87 μ_B was determined in solution, which corresponds to a tetrahedral coordination geometry.[24−27]

The bond distances are similar to those in **14** except for the Ni−P bond, which is 0.136 Å shorter. The folding of the ligand around the Ni−C13 hinge creates a rooflike

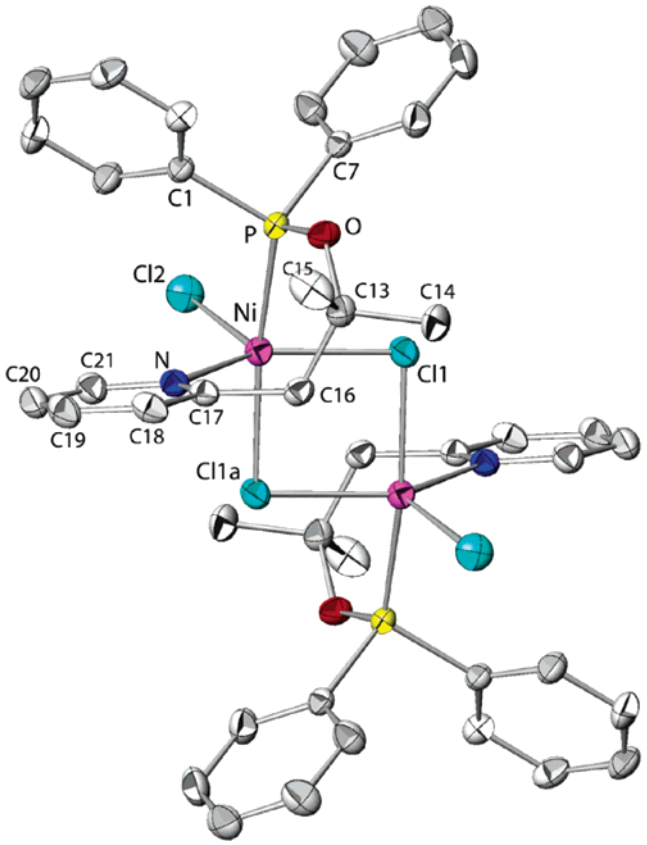

Figure 4. View of the molecular structure of **17** with thermal ellipsoids drawn at the 50% probability level.

Table 1. Characteristic Vibrations (cm^{-1}) for the Uncoordinated Phosphinitopyridines **11**−**13** and the Corresponding Ni(II) Complexes **15**−**17**

	$\nu_{C=C}$	ν_{cycle}	$\nu_{R\ sens}$	$\nu_{\beta(C-H)}$
ligand **11**	1569	996	695	1099
complex **15**	1599	1000, 1028	692	1107
ligand **12**	1573	997	696	1099
complex **16**	1604	1008, 1034	693	1112
ligand **13**	1569	997	695	1099
complex **17**	1602	1002, 1030	692	1105

Table 2. Selected Bond Lengths (Å) and Angles (deg) in **14**

Ni−P	2.2649(8)	P−O1	1.623(2)
Ni−N	1.987(2)	O1−C13	1.456(3)
Ni−Cl1	2.2229(7)	C13−C16	1.509(3)
Ni−Cl2	2.2078(9)	N−C16	1.285(3)
Cl1−Ni−Cl2	125.71(3)	P−Ni−N	91.30(7)
Cl1−Ni−P	109.87(3)	P−O1−C13	124.8(2)
Cl2−Ni−P	105.35(3)	O1−C13−C16	109.3(2)
Cl1−Ni−N	104.68(6)	C16−N−Ni	128.0(2)
Cl2−Ni−N	114.54(6)		

conformation, which generates a sort of cavity limited by one of the P−phenyl groups.

The X-ray structure of **16** also shows a distorted square-planar-coordination geometry of the Ni atom, which is slightly more distorted toward tetrahedral than that in **15** (Scheme 1 and Table 4).

(23) Pfeffer, M.; Braunstein, P.; Dehand, J. *Spectrochim. Acta, Part A* **1974**, *30*, 331−340.
(24) Sacconi, L.; Nannelli, P.; Nardi, N.; Campigli, U. *Inorg. Chem.* **1965**, *4*, 943−949.
(25) Venanzi, L. M. *J. Chem. Soc. A* **1958**, 719−724.
(26) Dori, Z.; Gray, H. B. *J. Am. Chem. Soc.* **1966**, *88*, 1394−1398.
(27) Frömmel, T.; Peters, W.; Wunderlich, H.; Kuchen, W. *Angew. Chem., Int. Ed. Engl.* **1993**, *32*, 907−909.

Table 3. Selected Bond Lengths (Å) and Angles (deg) in **15**

Ni−P	2.129(1)	P−O1	1.611(2)
Ni−N	1.928(2)	O1−C13	1.477(3)
Ni−Cl1	2.223(1)	C13−C16	1.531(4)
Ni−Cl2	2.161(1)	N−C16	1.355(3)
Cl1−Ni−Cl2	93.59(4)	P−Ni−N	85.49(7)
Cl1−Ni−P	173.62(3)	P−O1−C13	122.8(2)
Cl2−Ni−P	90.67(3)	O1−C13−C16	107.8(2)
Cl1−Ni−N	90.94(7)	C16−N−Ni	126.5(2)
Cl2−Ni−N	171.04(7)		

Scheme 1. Boat and Roof Conformations of the Six-Membered Chelate Rings in the Nickel Phosphinite Complexes **14**−**16**

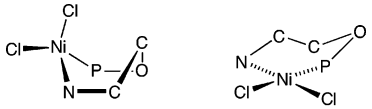

14

15, 16

Table 4. Selected Bond Lengths (Å) and Angles (deg) in **16**

Ni−P	2.123(2)	P−O	1.601(6)
Ni−N	1.916(7)	O−C13	1.476(9)
Ni−Cl1	2.167(2)	C13−C16	1.491(10)
Ni−Cl2	2.231(2)	N−C16	1.370(10)
Cl1−Ni−Cl2	95.08(9)	P−Ni−N	85.6(2)
Cl1−Ni−P	93.94(9)	P−O−C13	125.5(4)
Cl2−Ni−P	158.75(10)	O−C13−C16	108.8(6)
Cl1−Ni−N	164.8(2)	C16−N−Ni	124.8(5)
Cl2−Ni−N	90.6(2)		

Table 5. Selected Bond Lengths (Å) and Angles (deg) in **17**

Ni−P	2.362(1)	P−O	1.611(2)
Ni−N	2.041(2)	O−C13	1.470(2)
Ni−Cl1	2.367(1)	C13−C16	1.532(3)
Ni−Cl1a	2.418(1)	C16−C17	1.513(3)
Ni−Cl2	2.287(1)	N−C17	1.352(3)
Cl1−Ni−Cl2	109.95(4)	Cl1a−Ni−N	89.95(5)
Cl1a−Ni−Cl2	95.85(2)	Cl2−Ni−N	107.82(5)
Cl1a−Ni−Cl1	86.67(2)	P−Ni−N	85.37(5)
Cl1−Ni−P	90.00(2)	P−O−C13	129.1(1)
Cl1a−Ni−P	167.58(2)	O−C13−C16	115.1(2)
Cl2−Ni−P	96.53(2)	C13−C16−C17	119.3(2)
Cl1−Ni−N	142.23(6)	C17−N−Ni	117.4(1)

This increased distortion in **16** is assigned to the presence of the methyl substituent in the 6 position of the pyridine ring, although the Ni atom is in the mean plane passing through the atoms Cl1, Cl2, N, and P [distance of 0.0(3) Å]. The sum of the bond angles around Ni is 365.22°. Complex **16** shows a magnetic moment of 3.04 μ_B in solution, which corresponds to a tetrahedral-coordination sphere, as observed for compounds **14** and **15**.[24−27]

To examine the influence of an increased chelate ring size on the Ni-coordination sphere and the catalytic properties of the resulting complex, we prepared ligand **13** and its Ni(II) complex **17**. In contrast to complexes **14**−**16**, **17** is a centrosymmetric dinuclear complex with a pentacoordinated Ni(II) center (Figure 4 and Table 5). This underlines the considerable influence that the chelate ring size may exert on the coordination geometry of the metal. The metal is out of the N−Cl1−Cl2 plane by 0.004(1) Å and out of the P−Cl1−Cl2 plane by 0.021(1) Å. Its coordination sphere may be viewed as an intermediate between distorted square pyramidal and trigonal bipyramidal. In the former case, the base of the square pyramid is formed by the atoms P, N, Cl1, and Cl1a, with the Cl2 atom occupying the apical position. The Ni atom is out of this plane by 0.66(1) Å. In the latter description, the atoms N, Cl1, and Cl2 would form the basis of a trigonal bipyramid, with the Ni center being situated in their plane [distance of 0.004(1) Å]. In comparison to **14**−**16**, **17** exhibits slightly longer metal−ligand bond distances, which is related to its increased coordination number.

Magnetic moments of 2.67 (**14**), 2.87 (**15**), 3.04 (**16**), and 2.82 (**17**) μ_B were observed in solution using the Evans method.[29−31] Literature values for tetrahedral Ni(II) complexes are found in the range of 3.0−4.0 μ_B.[25,28−32] Our values are slightly different, but the magnetic moments of Ni(II) complexes strongly depend on the ligand field in which large differences can be observed.[25,26,28,32,33] Furthermore, equilibria between different structures may exist in solution.[26,27,33] For **17**, a change of the metal-coordination geometry from square pyramidal to tetrahedral most likely occurs in solution because a color change from ochre to violet is observed. Many tetrahedral Ni(II) complexes are blue/violet.[28]

Catalytic Ethylene Oligomerization with the Nickel(II) Phosphinite Complexes 14−**17.** The nickel(II) phosphinitooxazoline complex **14** and the nickel phosphinitopyridine complexes **15**−**17** were tested in the oligomerization of ethylene in order to examine the influence of the basicity of the nitrogen donor and the chelate ring size on the catalytic characteristics of the complexes. In the presence of methylalumoxane (MAO) or $AlEt_3$, complexes **14**−**17** were inactive. Only the formation of zerovalent nickel was observed. However, complexes **14**−**17** were active for ethylene oligomerization when 1.3, 2, or 6 equiv of $AlEtCl_2$ was used as a cocatalyst. For comparison, we also tested under the same conditions the complex $[NiCl_2(PCy_3)_2]$, a typical ethylene dimerization catalyst.[34]

For all of the catalytic tests, induction periods of ca. 3 min were observed. At the end of each catalysis, formation of a black precipitate was observed. In the presence of 1.3 equiv of $AlEtCl_2$, all complexes showed good activities except for $[NiCl_2(PCy_3)_2]$, which was inactive. For **14**−**17**, turnover frequencies of 11 600 (**14**), 11 600 (**15**), 23 300 (**16**), and 21 100 mol C_2H_4/(mol Ni)·h (**17**) were observed (Tables 6−9). These values increased when 2 equiv of the cocatalyst was used, and complexes **16** and **17** showed the highest turnover frequencies (Figure 5). For $[NiCl_2(PCy_3)_2]$, only a modest activity of 1600 mol C_2H_4/(mol Ni)·h was observed. Activities of 43 000 (**15**) and ca. 50 000 (**14**, **16**, and **17**) mol C_2H_4/(mol Ni)·h were obtained in the presence of 6 equiv of the cocatalyst (Figure 5).

(28) Holleman, A. F.; Wiberg, E. *Holleman-Wiberg Lehrbuch der Anorganischen Chemie*, 91−100 ed.; Walter de Gruyter: Berlin, 1985; pp 1152−1156.
(29) Evans, D. F. *J. Chem. Soc.* **1959**, 2003.
(30) Löliger, J.; Scheffold, R. *J. Chem. Educ.* **1972**, *49*, 646−647.
(31) Sur, S. K. *J. Magn. Reson.* **1989**, *82*, 169−173.
(32) Greenwood, N. N.; Earnshaw, A. *Chemistry of the Elements*; Pergamon Press: Oxford, 1984; pp 1337−1349.
(33) Hayter, R. G.; Humiec, F. S. *Inorg. Chem.* **1965**, *4*, 1701−1706.
(34) (a) Knudsen, R. D. *Prepr.—Am. Chem. Soc., Div. Pet. Chem.* **1989**, 572−576. (b) Commereuc, D.; Chauvin, Y.; Léger, G.; Gaillard, J. *Rev. Inst. Fr. Pet.* **1982**, *37*, 639−649.

Table 6. Ethylene Oligomerization with Precatalyst **14** Using $AlEtCl_2$ as the Cocatalyst, in 15[a] and 50 mL[b] of Toluene[c]

	14[a]			**14**[b]		
$AlEtCl_2$ (equiv)	6	2	1.3	6	2	1.3
selectivity C_4 (%)	64	81	92	82	87	91
selectivity C_6 (%)	33	18	8	16	13	9
selectivity C_8 (%)	3	1		2	0.1	
selectivity C_{10} (%)	0	0	0	0.2	0	0
productivity (g C_2H_4/(g Ni)·h)	23 600	14 000	5500	17 700	13 700	11 600
TOF (mol C_2H_4/(mol Ni)·h)	49 500	30 100	11 600	37 100	28 600	24 300
α-olefin (C_4) (%)	8	14	16	7	17	17

[a] Conditions: $T = 30$ °C, 10 bar of C_2H_4, 35 min, 4×10^{-2} mmol of Ni complex, solvent = 15 mL of toluene. [b] Conditions: $T = 30$ °C, 10 bar of C_2H_4, 35 min, 4×10^{-2} mmol of Ni complex, solvent = 50 mL of toluene. [c] No C_{12} oligomers were detected.

Table 7. Ethylene Oligomerization with Precatalyst **15** Using $AlEtCl_2$ as the Cocatalyst, in 15[a] and 50 mL of Toluene[b,c]

	15[a]			**15**[b]
$AlEtCl_2$ (equiv)	6	2	1.3	6
selectivity C_4 (%)	64	87	92	79
selectivity C_6 (%)	33	13	13	19
selectivity C_8 (%)	3	0.1	0.1	2
selectivity C_{10} (%)	0.1			0.2
productivity (g C_2H_4/(g Ni)·h)	20 900	7800	5500	18 500
TOF (mol C_2H_4/(mol Ni)·h)	43 700	16 300	11 600	38 700
α-olefin (C_4) (%)	5	18	19	7

[a] Conditions: $T = 30$ °C, 10 bar of C_2H_4, 35 min, 4×10^{-2} mmol of Ni complex, solvent = 15 mL of toluene. [b] Conditions: $T = 30$ °C, 10 bar of C_2H_4, 35 min, 4×10^{-2} mmol of Ni complex, solvent = 50 mL of toluene. [c] No C_{12} oligomers were detected.

Table 8. Ethylene Oligomerization with Precatalyst **16** Using $AlEtCl_2$ as the Cocatalyst[a,b]

$AlEtCl_2$ (equiv)	6	2	1.3
selectivity C_4 (%)	71	80	80
selectivity C_6 (%)	29	20	20
productivity (g C_2H_4/(g Ni)·h)	23 800	21 200	11 100
TOF (mol C_2H_4/(mol Ni)·h)	49 900	44 400	23 300
α-olefin (C_4) (%)	9	10	15

[a] Conditions: $T = 30$ °C, 10 bar of C_2H_4, 35 min, 4×10^{-2} mmol of Ni complex, solvent = 15 mL of toluene. [b] No C_8−C_{12} oligomers were detected.

Replacement of the oxazoline heterocycle with a pyridine led to significantly higher activities for complexes **16** and **17** only when either 1.3 or 2 equiv of $AlEtCl_2$ was used. No notable difference was observed in the presence of 6 equiv of the cocatalyst. Thus, an increase of the chelate ring size from six to seven membered leads to the formation of more active species in the presence of small amounts of $AlEtCl_2$. The influence of a larger chelate ring size on the catalytic activity remains however modest, which may be due to similar coordination polyhedra for **15**−**17** in solution.

Complexes **14**−**17** are very good dimerization catalysts with selectivities for C_4 products of 64−92% (**14**) (Figure 6). In all cases, the formation of C_6 oligomers was observed in the presence of 2 or 6 equiv of $AlEtCl_2$, whereas C_8 oligomers were also observed, although in small quantities, except with **16**, and C_{10} oligomers only with **14** and **15** as

Table 9. Ethylene Oligomerization with Precatalyst **17** Using $AlEtCl_2$ as the Cocatalyst[a,b]

$AlEtCl_2$ (equiv)	6	2	1.3
selectivity C_4 (%)	59	61	79
selectivity C_6 (%)	35	35	20
selectivity C_8 (%)	5	0	1
productivity (g C_2H_4/(g Ni)·h)	23 800	19 500	12 400
TOF (mol C_2H_4/(mol Ni)·h)	49 400	40 800	21 100
α-olefin (C_4) (%)	6	8	17
k_α[c]	0.33	0.31	0.22

[a] Conditions: $T = 30$ °C, 10 bar of C_2H_4, 35 min, 4×10^{-2} mmol of Ni complex, solvent = 15 mL of toluene. [b] No C_{10}−C_{12} oligomers were detected. [c] k_α = 1-hexene (mol)/1-butene (mol).

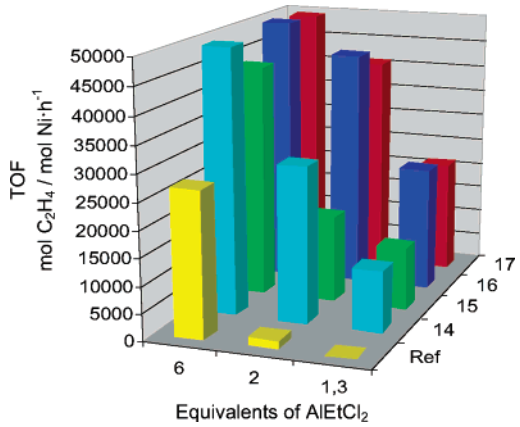

Figure 5. Activity of complexes **14**−**17** in the oligomerization of ethylene using different quantities of $AlEtCl_2$ as the cocatalyst. Conditions: $T = 30$ °C, 10 bar of C_2H_4, 35 min, 4×10^{-2} mmol of Ni, toluene (15 mL); ref = $[NiCl_2(PCy_3)_2]$.

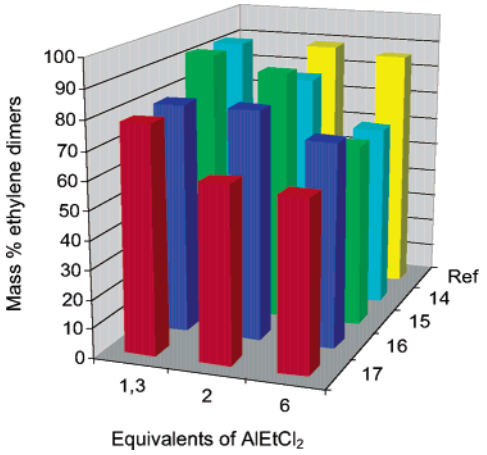

Figure 6. Selectivities of the complexes **14**−**17** for ethylene dimers. Conditions: $T = 30$ °C, 10 bar of C_2H_4, 35 min, 4×10^{-2} mmol of Ni, toluene (15 mL); ref = $[NiCl_2(PCy_3)_2]$.

catalysts. The phosphinitopyridine complex **16** with a more basic nitrogen donor showed a lower selectivity for ethylene dimers than complex **15** with 1.3 and 2 equiv of the cocatalyst (Figure 6). The behavior of **17** contrasts with that of **14** and **15**, which gave selectivities between 81 and 87% for the dimerization products in the presence of 2 equiv of the cocatalyst (Figure 6).

Complexes **14**−**17** led to selectivities for 1-butene of only 15−19% of the C_4 fraction in the presence of 1.3 equiv of the cocatalyst. This may be due to the exothermic character

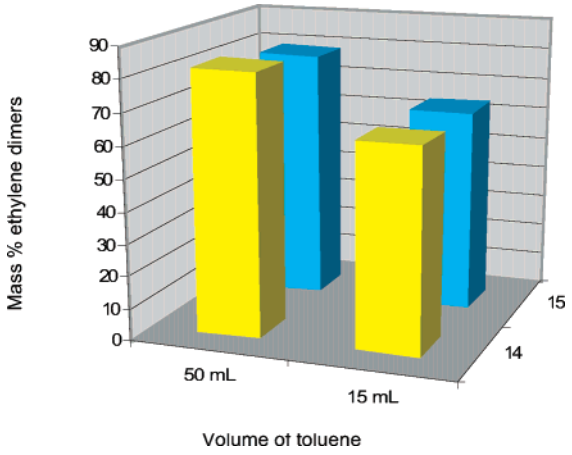

Figure 7. Selectivities of the complexes **14** and **15** for ethylene dimers in the presence of different quantities of solvent. Conditions: $T = 30$ °C, 10 bar of C_2H_4, 35 min, 4×10^{-2} mmol of Ni, 6 equiv of $AlEtCl_2$.

of the catalytic reactions, which favors isomerization to internal olefins.[35,36] Therefore, complexes **14** and **15** were tested using 50 mL instead of 15 mL of toluene as the solvent in order to better control the reaction temperature (Tables 6 and 7). The reactions were less exothermic (by about 10−15 °C), but no significant influence on the amount of 1-butene formed could be detected. Surprisingly, the product distribution with both complexes was shifted toward ethylene dimers (Figure 7). The turnover frequencies decreased by ca. 20% with 6 equiv of the cocatalyst but doubled in the case of **14** with 1.3 equiv of the cocatalyst.

The stability of the phosphinite ligands may be of concern in homogeneous catalysis. Such ligands may lead to Arbuzov rearrangement, while Smith and co-workers reported the rupture of a R−O bond in phosphates, phosphonates, and phosphites in the presence of organoaluminum compounds such as $AlEtCl_2$ and the resulting formation of the aluminum adduct **25** and alkyl or aryl chloride (eq 11).[37] For a given

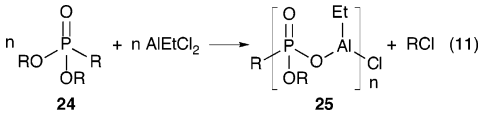

24 **25**

alkyl group, the ease of elimination decreased in the series as follows: $(RO)_2RPO/AlEtCl_2$ > $(RO)_3PO/AlEtCl_2$ > $(EtO)_3P/AlEtCl_2$. Therefore, we felt it necessary to test the stability of the phosphinite ligands using the diphenylphosphinitooxazoline **9** as an example. This ligand was reacted at room temperature with 1 equiv of $AlEtCl_2$ in toluene, and the reaction was followed by ^{31}P NMR spectroscopy. A singlet at 34.6 ppm indicates the formation of a phosphinite/$AlEtCl_2$ complex whose suggested structure **26** is shown below. After 3 days, slow decomposition of **26** was observed, and new ^{31}P NMR signals were observed between −10 and −17 ppm, which correspond to PPh_2Et species. The aluminum phosphinitooxazoline complex **26** was also tested as a

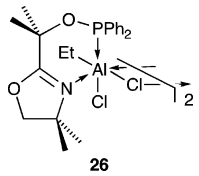

26

cocatalyst in the oligomerization of ethylene using **14** as a precatalyst in order to check whether the transfer of the phosphinite ligand **9** from the nickel complex to $AlEtCl_2$ would be the reason for the activity of complexes **14**−**17**. Using the same ratio of Al/Ni as in the other experiments, the activity observed in this test was very low, and the product distribution was shifted toward C_6 and C_8 oligomers when compared to the results obtained for the complex **14** under similar conditions. Therefore, we do not believe that the activation pathway involves direct interaction between the Ni-coordinated ligand and the $AlEtCl_2$ cocatalyst.

Conclusion

The new phosphinitooxazoline **9** and the phosphinitopyridine ligands **11**−**13** were prepared in good yields for the synthesis of the mononuclear **14**−**16** and dinuclear **17** Ni(II) complexes. These complexes were characterized by single-crystal X-ray diffraction in the solid state and in solution with the help of the Evans method, which indicated differences between the metal-coordination spheres in the solution and the solid state. These metal complexes were evaluated for the catalytic oligomerization of ethylene. In the presence of MAO and $AlEt_3$, only the decomposition of the Ni complexes was observed. However, complexes **14**−**17** provided activities up to 50 000 mol of C_2H_4/(mol of Ni)·h (**16** and **17**) in the presence of 6 equiv of $AlEtCl_2$. The selectivities for ethylene dimers were as high as 92% (**14** and **15**) in the presence of only 1.3 equiv of $AlEtCl_2$. The precatalysts **14**−**17** led to a selectivity for 1-butene of only 14−19%. The activities for **14**−**17** were superior to that of $[NiCl_2(PCy_3)_2]$, a typical dimerization catalyst, which was taken as a reference.[34]

At this stage, it is difficult to strictly relate the catalytic performances of a Ni(II) complex to its coordination geometry, in particular because structures intermediate between square planar and tetrahedral are often encountered. The subtle ligand or packing effects that may be responsible for these structural changes in the solid state cannot be easily extrapolated or do not apply to the structures in solution, and the latter are difficult if not impossible to assess in situ. Recent theoretical studies on the structures and energies of the transition states for the insertion of the C═C bond of various (functional) olefins into the metal−carbon bond of generic models for the Ni(II) and Pd(II) complexes with diimine (Brookhart) and salicylaldiminato (Grubbs) ligands have shown that nickel systems show lower insertion barriers than their palladium counterparts owing to their easier access to the required tetrahedral transition state.[38]

From the study of the phosphinite **9**/$AlEtCl_2$ system, we concluded that in our case ligand transfer from the nickel

(35) Brown, S. J.; Masters, A. F. *J. Organomet. Chem.* **1989**, *367*, 371−374.
(36) Abeywickrema, R.; Bennett, M. A.; Cavell, K. J.; Kony, M.; Masters, A. F.; Webb, A. G. *J. Chem. Soc., Dalton Trans.* **1993**, 59−68.
(37) Cohen, B. M.; Smith, J. D. *J. Chem. Soc. A* **1969**, 2087−2089.
(38) Deubel, D. V.; Ziegler, T. *Organometallics* **2002**, *21*, 4432−4441.

atom to the aluminum cocatalyst is unlikely to represent an activation mechanism.

Experimental Section

General Procedures. All solvents were dried and distilled using common techniques unless otherwise stated. $NiCl_2 \cdot 6H_2O$ was dried by heating for 6 h at 160 °C under vacuum to afford anhydrous $NiCl_2$. $NiX_2(DME)$ (X = Cl, Br),[39] **18**,[18] and 2-bromo-6-methylpyridine[19] were prepared according to the literature. Other chemicals were commercially available and were used without further purification unless otherwise described. The ^1H, $^{31}P\{^1H\}$, and $^{13}C\{^1H\}$ NMR spectra were recorded at 500.13 or 300.13, 121.5, and 76.0 MHz, respectively, on FT Bruker AC300, Avance 300, or Avance 500 instruments. IR spectra in the range of 4000−400 cm^{-1} were recorded on Bruker IFS66FT and Perkin-Elmer 1600 Series FTIR instruments. Gas chromatographic analyses were performed on a Thermoquest GC8000 Top Series gas chromatograph using a HP Pona column (50 m, 0.2 mm diameter, 0.5 μm film thickness). For all complexes whose magnetic moments were determined with the help of the Evans method, a $CH_3NO_2-CD_2Cl_2$ solution (80:20, v/v) was used as the reference. The solvents were degassed and dried using standard techniques. For a standard NMR experiment, a 0.055−0.10 M solution of the paramagnetic substance in CD_2Cl_2 was prepared.

Preparation of 4,4-Dimethyl-2-[1-oxy(diphenylphosphine)-1-methylethyl]-4,5-dihydrooxazole (9). The oxazoline alcohol[18] **18** (1.083 g, 6.89 mmol) was dissolved in THF (50 mL), and the solution was cooled to −78 °C before 1 equiv of *n*-BuLi (1.6 M solution in hexanes, 4.30 mL, 6.89 mmol) was slowly added. After the reaction mixture was stirred for 1 h at −78 °C, 1.0 equiv of PPh_2Cl (1.52 g, 1.3 mL, 6.89 mmol) was added. The solution was further stirred for 2 h at −78 °C before it was brought to room temperature overnight. The reaction mixture was hydrolyzed by the addition of degassed water (10 mL), and the organic phase was separated. The aqueous phase was extracted twice with diethyl ether (20 mL). The organic phase was dried over $MgSO_4$ and filtered. The solvent was evaporated under reduced pressure, yielding the product as a white oil (1.78 g, 6.89 mmol, 76%). IR (CH_2Cl_2): 1661 cm^{-1}. ^1H NMR ($CDCl_3$) δ: 1.27 (s, 6H, $C(CH_3)_2$), 1.64 (s, 6H, $OC(CH_3)_2$), 3.75 (s, 2H, OCH_2), 7.28−7.51 (m, 10H, PPh_2). $^{13}C\{^1H\}$ NMR ($CDCl_3$) δ: 26.5 (s, $NC(CH_3)_2$), 28.1 (s, $OC(CH_3)_2$), 67.3 (s, $NC(CH_3)_2$), 75.4 (s, $OC(CH_3)_2$), 79.0 (s, OCH_2), 128.0−131.7 (m, PPh_2), 167.2 (s, C=N). $^{31}P\{^1H\}$ NMR ($CDCl_3$) δ: 95.4 (s). Anal. Calcd for $C_{20}H_{24}NO_2P$: C, 70.37; H, 7.09; N, 4.10. Found: C, 70.61; H, 7.32; N, 4.23.

Preparation of 4,4-Dimethyl-2-[1-oxy(diisopropylphosphine)-1-methylethyl]-4,5-dihydrooxazole (10). The oxazoline alcohol **18**[18] (1.96 g, 12.5 mmol) was dissolved in 50 mL of toluene, and 3 equiv of NEt_3 (3.79 g, 5.2 mL, 37.5 mmol) was added. After the reaction mixture was cooled to 0 °C, 1.0 equiv of $P(BH_3)(i\text{-}Pr)_2Cl$ (1.92 g, 2.0 mL, 12.5 mmol) was added. The solution was further stirred for 30 min at 0 °C before it was brought to room temperature. After 1 h, the formation of a white precipitate was observed. The reaction mixture was stirred for 10 h at room temperature before the solution was filtered through Celite. The Celite was washed twice with toluene (20 mL). The organic fractions were pooled and evaporated under reduced pressure, yielding a transparent oil.

To deprotect the phosphinite **22**, it was dissolved in 30 mL of degassed $NHEt_2$ and stirred for 10 h. After all volatiles were evaporated, only the decomposition of the phosphinitooxazoline was observed.

(39) Cotton, F. A. *Inorg. Synth.* **1971**, *13*, 160−164.

Preparation of 2-Ethyl-[1′-methyl-1′-oxy(diphenylphosphino)]-pyridine (11). A solution of the pyridine alcohol **21** (1.73 g, 13 mmol) in 30 mL of THF was cooled to −78 °C and stirred for 30 min before 1 equiv of *n*-BuLi (1.6 M solution in hexanes, 8.13 mL, 13 mmol) was slowly added. After the solution was stirred for 1 h at −78 °C, 1 equiv of PPh_2Cl (2.30 mL, 2.78 g, 13 mmol) was added. The reaction mixture was brought to room temperature overnight and then hydrolyzed by the addition of degassed water (10 mL). The organic phase was separated, and the aqueous phase was extracted twice with diethyl ether (20 mL). The organic fractions were dried over $MgSO_4$, filtered, and taken to dryness under reduced pressure, yielding the product as a transparent oil (3.81 g, 12 mmol, 91%). ^1H NMR ($CDCl_3$) δ: 1.79 (s, 3H, $C(CH_3)_2$), 7.14 (m, 1H, py−H^5), 7.34 (d, 1H, py−H^3, $^3J(H^3,H^4)$ = 8.1 Hz), 7.35−7.50 (m, 10H, PPh_2), 7.65 (m, 1H, py−H^4), 8.50 (d, 1H, py−H^6, $^3J(H^6,H^5)$ = 8.1 Hz). $^{13}C\{^1H\}$ NMR ($CDCl_3$) δ: 28.4 (s, $C(CH_3)_2$), 80.0 (s, $C(CH_3)_2$), 114.8 (s, py−C^5), 120.0 (s, py−C^3), 126.6 (d, Ph−C_o, ^2J(P,C) = 12.5 Hz), 127.3 (s, P−Ph_m), 128.8 (d, P−C_{ipso}, ^1J(P,C) = 25.0 Hz), 130.0 (s, Ph−C_p), 135.2 (s, py−C^4), 150.2 (s, py−C^6), 163.7 (s, py−C^2). $^{31}P\{^1H\}$ NMR ($CDCl_3$) δ: 89.3 (s). Anal. Calcd for $C_{20}H_{20}NOP$: C, 74.75; H, 6.27; N, 4.36. Found: C, 74.32; H, 6.20; N, 4.30.

Preparation of 2-Ethyl-6-methyl-[1′-methyl-1′-oxy(diphenylphosphino)]pyridine (12). A solution of the pyridine alcohol **22** (1.79 g, 12 mmol) in 60 mL of THF was cooled to −78 °C, and 1 equiv of *n*-BuLi (1.6 M solution in hexanes, 7.4 mL, 12 mmol) was slowly added. After the solution was stirred for 1 h at −78 °C, 1 equiv of PPh_2Cl (2.64 g, 2.20 mL, 12 mmol) was added. The reaction conditions and workup are similar to those for **11**, yielding the product as a transparent viscous liquid, which solidified upon standing (5.7 g, 17 mmol, 85%). ^1H NMR ($CDCl_3$) δ: 1.78 (s, 6H, $C(CH_3)_2$), 2.48 (s, 3H, py−CH_3), 7.00 (d, 1H, py−H^5, ^3J(H,H) = 7.8 Hz), 7.10 (d, 1H, py−H^3, $^3J(H^3,H^4)$ = 7.8 Hz), 7.20−7.30 (m, 10H, PPh_2), 7.50 (t, 1H, py−H^4, ^3J(H,H) = 7.8 Hz). $^{13}C\{^1H\}$ NMR ($CDCl_3$) δ: 23.1 (s, py−CH_3), 28.4 (s, $C(CH_3)_2$), 80.0 (s, $C(CH_3)_2$), 114.8 (s, py−C^5), 120.0 (s, py−C^3), 126.6 (d, Ph−C_o, ^2J(P,C) = 15.5 Hz), 127.3 (s, Ph−C_m), 128.8 (d, Ph−C_{ipso}, ^1J(P,C) = 25.6 Hz), 130.0 (s, P−C_p), 135.2 (s, py−C^4), 150.2 (s, py−C^5), 163.7 (s, py−C^2). $^{31}P\{^1H\}$ NMR ($CDCl_3$) δ: 88.8 (s). Anal. Calcd for $C_{21}H_{22}NOP$: C, 75.21; H, 6.61; N, 4.18. Found: C, 75.55; H, 7.00; N, 4.25.

Preparation of 2-Propyl-[2′-methyl-2′oxy(diphenylphosphino)]pyridine (13). A solution of the pyridine alcohol **23** (3.0 g, 20 mmol) in 60 mL of THF was cooled to −78 °C, and 1 equiv of *n*-BuLi (1.6 M solution in hexanes, 12.4 mL, 20 mmol) was slowly added. After the solution was stirred for 1 h at −78 °C, 1 equiv of PPh_2Cl (4.4 g, 3.70 mL, 20 mmol) was added. The reaction conditions and workup were similar to those for **11**, yielding the product as a transparent viscous liquid, which solidified upon standing (5.7 g, 17 mmol, 85%). ^1H NMR ($CDCl_3$) δ: 1.42 (s, 6H, $C(CH_3)_2$), 3.19 (s, 2H, py−CH_2), 7.12 (t, 1H, py−H^5, $^3J(H^5,H^{6,4})$ = 7.8 Hz), 7.30 (m, 1H, py−H^3), 7.20−7.30 (m, 10H, PPh_2), 7.75 (d, 1H, py−H^4, $^3J(H^4,H^{5,3})$ = 7.8 Hz), 8.51 (d, 1H, py−H^6, $^3J(H^6,H^5)$ = 7.8 Hz. $^{13}C\{^1H\}$ NMR ($CDCl_3$) δ: 26.5 (s, $C(CH_3)_2$), 49.9 (s, py−CH_2), 69.2 (s, $C(CH_3)_2$), 119.9 (s, py−C^5), 124.0 (s, py−C^3), 126.6 (d, Ph−C_o, ^2J(P,C) = 16.5 Hz), 127.3 (s, Ph−C_m), 128.6 (d, Ph−C_{ipso}, ^1J(P,C) = 22.3 Hz), 130.0 (s, Ph−C_p), 136.0 (s, py−C^4), 147.0 (s, py−C^5), 164.0 (s, py−C^2). $^{31}P\{^1H\}$ NMR ($CDCl_3$) δ: 88.8 (s). Anal. Calcd for $C_{21}H_{22}NOP$: C, 75.21; H, 6.61; N, 4.18. Found: C, 74.75; H, 6.10; N, 3.95.

Preparation of [Nickel{1-[4,4-dimethyl-2-[1-oxy(diphenylphosphino)-1-methylethyl]]-4,5-dihydrooxazole} Dichloride] (14). To

a solution of the phosphinitooxazoline **9** (1.01 g, 2.97 mmol) in CH_2Cl_2 (30 mL) was added 0.9 equiv of [$NiCl_2$(DME)] (0.582 g, 2.67 mmol), and the reaction mixture was stirred for 2 h at room temperature. After 15 min, a color change from orange to violet was observed. The solution was then filtered through Celite to separate unreacted [$NiCl_2$(DME)], and the Celite was washed with CH_2Cl_2 (30 mL). The organic phases were pooled, and the solvent was evaporated. The violet solid was dissolved in 20 mL of toluene and precipitated by the addition of hexane (40 mL). The violet precipitate was allowed to settle, and the supernatant organic phase was separated with a glass pipet. The solid was taken to dryness under reduced pressure and dried under vacuum for 10 h, yielding a violet powder (1.04 g, 2.27 mmol, 75%). IR (CH_2Cl_2): 1630 cm^{-1} ($\nu_{C=N}$). Anal. Calcd for $C_{20}H_{24}Cl_2NNiO_2P$: C, 51.00; H, 5.14; N, 2.97. Found: C, 50.80; H, 4.85; N, 2.79.

Preparation of [Nickel{2-ethyl-[1′-methyl-1′-oxy(diphenylphosphino)]pyridine} Dichloride] (15). To a solution of the phosphinitopyridine **11** (0.896 g, 2.78 mmol) in CH_2Cl_2 (30 mL) was added 0.9 equiv of [$NiCl_2$(DME)] (0.546 g, 2.50 mmol), and the reaction mixture was stirred for 2 h at room temperature. After 15 min, a color change from orange to brick red was observed. The reaction conditions and workup were similar to those for **14**, affording a violet solid, which was dissolved in 20 mL of toluene and precipitated by the addition of hexane (40 mL). The supernatant organic phase was separated, and the solid was dried under vacuum for 12 h, yielding a brick-red powder (0.77 g, 1.69 mmol, 68%). ^{1}H NMR ($CDCl_3$) δ: 2.58 (s, vbr, 6H, C(CH_3)$_2$), 7.1−9.1 (5 s, vbr, 14H, 4(py−H), 10 PPh_2). Anal. Calcd for $C_{20}H_{20}Cl_2NNiOP$: C, 53.27; H, 4.47; N, 3.11. Found: C, 52.93; H, 4.49; N, 2.87.

Preparation of [Nickel{2-ethyl-6-methyl-[1′-methyl-1′-oxy-(diphenylphosphino)]pyridine} Dichloride] (16). To a solution of the phosphinitopyridine **12** (1.420 g, 4.23 mmol) in CH_2Cl_2 (40 mL) was added 0.9 equiv of [$NiCl_2$(DME)] (0.830 g, 3.81 mmol), and the reaction mixture was stirred for 2 h at room temperature. After 15 min, a color change from orange to violet was observed. The reaction conditions and workup were similar to those for **14**, affording a violet solid, which was dissolved in 20 mL of toluene and precipitated by the addition of hexane (40 mL). The supernatant organic phase was separated, and the solid was dried under vacuum for 12 h, yielding a violet-red powder (1.39 g, 2.99 mmol, 79%). ^{1}H NMR ($CDCl_3$) δ: 3.01 (s, 6H, C(CH_3)$_2$), 5.28 (s, 3H, py−CH_3) 7.2−7.8 (m, 13H, 3(py−H), 10 PPh_2). Anal. Calcd for $C_{21}H_{22}Cl_2$-NNiOP: C, 54.24; H, 4.77; N, 3.01. Found: C, 52.51; H, 4.95; N, 2.82.

Preparation of [Nickel{2-propyl-[2′-methyl-2′-oxy(diphenylphosphino)]pyridine} Dichloride]$_2$ (17). To a solution of the phosphinitopyridine **13** (1.212 g, 3.62 mmol) in CH_2Cl_2 (40 mL) was added 0.9 equiv of [$NiCl_2$(DME)] (0.769 g, 3.50 mmol), and the reaction mixture was stirred for 2 h at room temperature. After 15 min, a color change from orange to violet was observed. The reaction conditions and workup were similar to those for **14**, affording a violet solid, which was dissolved in 20 mL of toluene and precipitated by the addition of hexane (40 mL). The supernatant organic phase was separated, and the solid was dried under vacuum for 12 h, yielding an ochre-colored powder (1.26 g, 2.72 mmol, 75%). Anal. Calcd for $C_{42}H_{44}Cl_4N_2Ni_2O_2P_2$: C, 54.24; H, 4.77; N, 3.01. Found: C, 54.00; H, 4.95; N, 3.15.

Preparation of 2-Pyridin-2-ylpropan-2-ol (21). A solution of 2-bromopyridine[19] (11.0 mL, 17.87 g, 113 mmol) in 100 mL of THF was cooled to −78 °C and stirred for 30 min before 1 equiv of *n*-BuLi (1.6 M solution in hexanes, 70.71 mL, 113 mmol) was slowly added over a period of 15 min. The reaction mixture was stirred for 2 h at −78 °C before 40 mL of distilled acetone was added, and the solution was brought to room temperature overnight. After 4 h, the formation of an orange precipitate was observed. The reaction mixture was hydrolyzed by transferring it into a saturated NH_4Cl solution (200 mL). The organic phase was separated, and the aqueous phase was extracted twice with diethyl ether (200 mL). The organic fractions were collected and dried over Na_2SO_4. After filtration, the solvent was evaporated, and the remaining orange-brown oil was distilled under vacuum (2 Torr, 45 °C), yielding a transparent liquid (9.30 g, 67 mmol, 60%). ^{1}H NMR ($CDCl_3$) δ: 1.53 (s, 6H, C(CH_3)$_2$), 5.0 (s, 1H, OH), 7.14 (m, 1H, py−H^5), 7.34 (d, 1H, py−H^3, $^3J(H^3,H^4)$ = 8.1 Hz), 7.65 (m, 1H, py−H^4), 8.50 (d, 1H, py−H^6, $^3J(H^5,H^6)$ = 8.1 Hz). These data are consistent with the literature values.[20,22]

Preparation of 2-(6-Methylpyridin-2-yl)propan-2-ol (22). A solution of 2-bromo-6-methylpyridine[19] (19.66 g, 114 mmol) in 150 mL of THF was cooled to −78 °C and stirred for 30 min before 1 equiv of *n*-BuLi (1.6 M solution in hexanes, 71.40 mL, 114 mmol) was slowly added over a period of 15 min. The reaction conditions and workup were similar to those for **21**, yielding an orange-brown oil that was distilled under vacuum (2 Torr, 75 °C) to afford a transparent liquid (12.08 g, 80 mmol, 70%). ^{1}H NMR ($CDCl_3$) δ: 1.56 (s, 6H, C(CH_3)$_2$), 2.53 (s, 3H, py−CH_3), 5.58 (s, 1H, OH), 7.00 (d, 1H, py−H^3, ^3J(H,H) = 7.8 Hz), 7.10 (d, 1H, py−H^5, ^3J(H,H) = 7.8 Hz), 7.57 (t, 1H, py−H^4, ^3J(H,H) = 7.8 Hz). These data are consistent with the literature values.[20,22]

Preparation of 2-Methyl-1-pyridin-2-ylpropan-2-ol (23). A solution of α-picoline (21.20 g, 230 mmol) in 200 mL of THF was cooled to −78 °C and stirred for 30 min before 1 equiv of *n*-BuLi (1.6 M solution in hexanes, 142.0 mL, 230 mmol) was slowly added over a period of 30 min. The reaction conditions and workup were similar to those for **21**, affording an orange-brown oil that was distilled under vacuum (2 Torr, 60 °C) to give a transparent liquid (24.67 g, 163 mmol, 71%). ^{1}H NMR ($CDCl_3$) δ: 1.21 (s, 6H, C(CH_3)$_2$), 2.92 (s, 2H, CH_2), 5.60 (s, 1H, OH), 7.1 (d, 1H, py−H^3, ^3J(H,H) = 7.7 Hz), 7.12 (d, 1H, py−H^5, ^3J(H,H) = 7.7 Hz), 7.65 (t, 1H, py−H^4, ^3J(H,H) = 7.8 Hz), 8.53 (m, 1H, py−H^6). These data are consistent with the literature values.[40]

Oligomerization of Ethylene. All catalytic reactions were carried out in a magnetically stirred (900 rpm) 100 mL stainless-steel autoclave. The interior of the autoclave was protected from corrosion by a protective coating. All catalytic tests were started at 30 °C, and no cooling of the reactor was done during the reaction. After injection of the catalyst solution under a constant low flow of ethylene, the reactor was pressurized to the desired pressure. The temperature increase that was observed resulted solely from the exothermicity of the reaction. When the alkylaluminum compounds were used as cocatalysts, the activator was also injected under a constant ethylene flow and finally brought to working pressure. The reactor was continuously fed with ethylene by a reserve bottle placed on a balance to allow continuous monitoring of the ethylene uptake. In all of the catalytic experiments with MAO and $AlEtCl_2$, 4.0×10^{-2} mmol of the Ni complex were used. The oligomerization products and remaining ethylene were only collected from the reactor at the end of the catalytic experiment. At the end of each test, the reactor was cooled to 10 °C before transferring the gaseous phase into a 10 L polyethylene tank filled with water. An aliquot of this gaseous phase was transferred into a Schlenk flask, previously evacuated for GC analysis. The products in the reactor were hydrolyzed in situ by the addition of ethanol (10 mL), transferred in a Schlenk flask, and separated from the

(40) Koning, B.; Buter, J.; Hulst, R.; Stroetinga, R.; Kellogg, R. M. *Eur. J. Org. Chem.* **2000**, *15*, 2735−2743.

Table 10. Crystallographic Data for Complexes **14**−**17**

	14	**15**	**16**	**17**
formula	$C_{20}H_{24}Cl_2NNiO_2P$	$C_{20}H_{20}Cl_2NNiOP$	$C_{21}H_{22}Cl_2NNiOP$	$C_{42}H_{44}Cl_4N_2Ni_2O_2P_2$
fw	470.98	450.95	464.98	929.95
crystal system	monoclinic	triclinic	monoclinic	triclinic
space group	$P2_1/c$	$P\bar{1}$	$P2_1/n$	$P\bar{1}$
a (Å)	8.999(2)	9.151(5)	10.2634(3)	9.267(5)
b (Å)	14.579(2)	10.262(5)	16.9550(5)	9.280(5)
c (Å)	16.535(2)	11.874(5)	11.8716(4)	13.987(5)
V (Å^3)	2166.0(6)	1020.4(9)	2045.34(11)	1038.2(9)
α (deg)	90	99.29(1)	90	96.05(1)
β (deg)	93.16(5)	108.43(1)	98.08(1)	94.42(1)
γ (deg)	90	98.44(1)	90	118.67(1)
Z	4	2	4	1
color	violet	red	violet	ochre
crystal size, mm	0.10 × 0.10 × 0.08	0.10 × 0.10 × 0.08	0.10 × 0.10 × 0.08	0.11 × 0.14 × 0.08
D_{calcd} (g·cm^{-3})	1.444	1.468	1.510	1.487
μ (mm^{-1})	1.231	1.300	1.299	1.280
θ limits (deg)	1.86/27.49	1.85/27.52	2.11/27.51	2.54/34.99
no. of data measured	4950	4645	4659	9028
no. of data with $I > 2\sigma(I)$	3521	3774	3521	6146
no. of variables	245	235	245	245
R	0.0369	0.0357	0.0888	0.0677
R_w	0.0803	0.1109	0.2310	0.0973
GOF on F^2	1.015	1.073	1.176	1.093

metal complexes by trap-to-trap distillation (120 °C, 20 Torr). All volatiles were evaporated (120 °C, 20 Torr static pressure) and recovered in a second flask previously immersed in liquid nitrogen in order to avoid any loss of product. For GC analyses, 1-heptene was used as an internal reference. The necessary amount of complex for six catalytic runs was dissolved in 60 mL of toluene. For each catalysis, 10 mL of this solution was injected into the reactor. Depending on the amount of cocatalyst added, between 0 and 5 mL of the solvent was added so that the total volume of all of the solutions was 15 mL. This can be summarized by the following equation:

$$10\ \text{mL (Ni solution)} + y\ \text{mL (solvent)} + z\ \text{mL (cocatalyst solution)} = 15\ \text{mL}$$

When MAO was used as the cocatalyst, the total volume was increased to 20 mL.

X-ray Structure Determinations of 14−**17.** Diffraction data were collected at 180 K on a Kappa CCD diffractometer using graphite-monochromatized Mo Kα radiation ($\lambda = 0.710\ 73$ Å) and a ϕ-scan mode. The relevant data are summarized in Table 10. Data were collected using ϕ scans, and the structures were solved by direct methods using the SHELX-97 software.[41,42] The refinements were conducted by full-matrix least squares on F^2. No absorption correction was used. All non-hydrogen atoms were refined anisotropically with H atoms mathematically introduced as fixed contributors (*SHELXL procedure*). Full data-collection parameters and structural data are available as the Supporting Information. Crystallographic data for all of the structures in this paper have been deposited with the Cambridge Crystallographic Data Centre, CCDC 224957-224960. Copies of this information may be obtained free of charge from The Director, CCDC, 12 Union Road, Cambridge CB2 1EZ, U.K. (fax, +44 1223 336033; e-mail, deposit@ccdc.cam.ac.uk; web, http://www.ccdc.cam.ac.uk).

Acknowledgment. We are grateful to the CNRS and the Ministère de la Recherche (Paris) for support and to the Institut Français du Pétrole for a Ph.D. grant (F.S.) and financial support.

Supporting Information Available: X-ray data for **14**−**17** available in CIF format and ORTEP plots of all of the structures with complete atom numbering. This material is available free of charge via the Internet at http://pubs.acs.org.

IC035132I

(41) *Kappa CCD Operation Manual*; Nonius B. V.: Delft, The Netherlands, 1997.

(42) Sheldrick, G. M. *SHELXL-97: Program for the Refinement of Crystal Structures*; University of Göttingen: Göttingen, Germany, 1997.